



HAL
open science

Are regional groundwater models suitable for simulating wetlands, rivers and intermittence? The example of the French AquifR platform

Luca Guillaumot, Simon Munier, Ronan Abhervé, Jean-Pierre Vergnes, Alexis Jeantet, Patrick Le Moigne, Florence Habet

► To cite this version:

Luca Guillaumot, Simon Munier, Ronan Abhervé, Jean-Pierre Vergnes, Alexis Jeantet, et al.. Are regional groundwater models suitable for simulating wetlands, rivers and intermittence? The example of the French AquifR platform. *Journal of Hydrology*, 2024, 644, pp.132019. 10.1016/j.jhydrol.2024.132019 . hal-04710029

HAL Id: hal-04710029

<https://hal.science/hal-04710029v1>

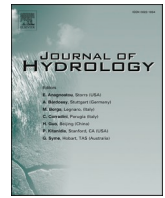
Submitted on 26 Sep 2024

HAL is a multi-disciplinary open access archive for the deposit and dissemination of scientific research documents, whether they are published or not. The documents may come from teaching and research institutions in France or abroad, or from public or private research centers.

L'archive ouverte pluridisciplinaire **HAL**, est destinée au dépôt et à la diffusion de documents scientifiques de niveau recherche, publiés ou non, émanant des établissements d'enseignement et de recherche français ou étrangers, des laboratoires publics ou privés.



Distributed under a Creative Commons Attribution 4.0 International License



Research papers

Are regional groundwater models suitable for simulating wetlands, rivers and intermittence? The example of the French AquIFR platform

Luca Guillaumot^{a,b,*}, Simon Munier^a, Ronan Abhervé^{c,d}, Jean-Pierre Vergnes^b, Alexis Jeantet^a, Patrick Le Moigne^a, Florence Habets^e

^a CNRM, Université de Toulouse, Météo-France, CNRS, Toulouse, France

^b Water, Environment, Processes and Analyses Division, BRGM – French Geological Survey, Orléans, France

^c Centre for Hydrology and Geothermics (CHYN), Université de Neuchâtel, Neuchâtel, Switzerland

^d Univ Rennes/CNRS, Géosciences Rennes, 263 Av. Général Leclerc, 35042 Rennes, France

^e Ecole Normale Supérieure, Institut Pierre Simon Laplace, CNRS, 75005 Paris, France

ARTICLE INFO

This manuscript was handled by Huaming Guo, Editor-in-Chief, with the assistance of Yueqing Xie, Associate Editor

Keywords:

Groundwater model
Groundwater-surface interactions
Wetland
River network
Intermittence

ABSTRACT

Predicting and managing water resources at regional scale under different climate and socio-economic scenarios is crucial to support drinking water supply and other sectors. At the same time, protecting rivers and wetlands from pollutions and droughts is essential and must include groundwater given its contribution to surface water. Yet, assessing temporal and spatial variability of groundwater contributions to surface water is constrained due to limited observations. This study aims to quantify the spatio-temporal distribution of groundwater discharge (hereafter called “GW discharge”) zones, i.e. the groundwater flow to rivers and wetlands, estimated by calibrated regional groundwater flow models (French AquIFR platform). We compare simulation results with two types of surface observations: (i) the spatial distribution of surface water (BD TOPO, RAMSAR and Natura 2000 database) and (ii) an innovative datasets, the river intermittence observed in headwaters (ONDE network). Results show that simulated GW discharge zones are consistent with the observed location of rivers and wetlands. Time variations in GW discharge are well correlated with the intermittence observed at 396 of the 515 selected stations. Of these, groundwater model continues to feed surface water upstream of the station for ~75 % of observed river drying up events, which may be consistent with a small alluvial flow. The groundwater withdrawals are shown to have a strong impact on the GW discharge and thus on the river intermittence.

1. Introduction

Groundwater recharge occurs when soil is moist enough so that water can flow, during humid and cold season, when precipitation exceeds evapotranspiration (Jasechko et al., 2014; Sobaga et al., 2023a), or locally by surface waters infiltration (Thierion et al., 2012). In the opposite, groundwater flows continuously and reaches rivers, lakes, seas, wetlands and root zone (Fan, 2015; Loheide and Gorelick, 2007; Martínez-de la Torre and Miguez-Macho, 2019; Maxwell and Condon, 2016; Taniguchi et al., 2002; Vergnes et al., 2014).

In France, groundwater supports two-thirds of drinking water and one-third of agricultural withdrawals (Pasquier, 2017). Groundwater resources are localized in sedimentary, fractured-weathered, alluvial or karstic aquifers (BRGM, 2022). Based on satellite gravimetric anomalies, and consistently with local lysimeter data, mainland France lost ~2–3

mm/yr of groundwater storage between 2002 and 2021 (Scanlon et al., 2023; Sobaga et al., 2023b; Xanke and Liesch, 2022). However, studies focusing on historical groundwater levels data faced difficulties in attributing climate and human contributions (Baulon et al., 2022; Boé and Habets, 2014; Cuthbert et al., 2019; Haas and Birk, 2019; Habets et al., 2013).

River intermittence is a critical process for ecosystems health (Busch et al., 2020; Costigan et al., 2016; Detry et al., 2014; Fovet et al., 2021). Furthermore, non-perennial rivers predominate worldwide (Messenger et al., 2021). Yet, river intermittence should increase in the context of global change (Sauquet et al., 2021; Trambly et al., 2021), as well as in wetlands (Armandine Les Landes et al., 2014; Zedler and Kercher, 2005). There is evidence from direct observations that river intermittence has increased in France (National Agency for Biodiversity (OFB), 2023; Nowak and Michon, 2017). Groundwater level appears as the

* Corresponding author at: 3 Av. Claude Guillemin, 45060 Orléans CEDEX 2, France.

E-mail address: l.guillaumot@brgm.fr (L. Guillaumot).

main factor controlling river intermittence (Condon and Maxwell, 2019; Jasechko et al., 2021; Sanz et al., 2011; Sophocleous, 2000; Winter, 1999), excepted where upstream flow exceeds river losses (mostly in arid or mountainous regions) (Costigan et al., 2016; Godsey and Kirchner, 2014; Shanafield et al., 2021). In this context, linking groundwater to surface water variability appears essential to decipher human impact on surface water (Bouwer and Maddock, 1997; de Graaf et al., 2019; Howard and Merrifield, 2010; Scanlon et al., 2023).

Quantifying groundwater recharge and the resulting groundwater contribution to rivers (Cornette et al., 2022; Hartmann et al., 2021; Rousset et al., 2004; Schuite et al., 2019; Simon et al., 2022) at basin or aquifer scale is still challenging. A relevant approach consists in modelling hydrological systems through flow equations (Maxwell et al., 2015; Therrien et al., 2010). Within these models, groundwater discharge (hereafter called “GW discharge”) supports surface water bodies where groundwater levels exceed surface water levels. However, in regional application, the assessment of groundwater models usually relies on sparse groundwater levels monitoring, while the groundwater contribution in observed river gauges stations is difficult to assess (Gleeson et al., 2021; Guillaumot et al., 2022).

Few groundwater modelling studies at catchment scale focus on river distribution (Abhervé et al., 2023; Barclay et al., 2020; Bresciani et al., 2016; Luo et al., 2010; Stoll and Weiler, 2010) or wetlands (Batelaan et al., 2003; Blazkova et al., 2002; Enemark et al., 2018; Franks et al., 1998; Grabs et al., 2009; Güntner et al., 2004; Vergnes and Habets, 2018). Meanwhile, simulating river intermittence with physically-based models is still a challenge (Blöschl et al., 2019; Zimmer and McGlynn, 2017). Authors such as Godsey and Kirchner (2014) and Abhervé et al.

(2023) have argued the potential of observations of river network expansion and contraction to inform on subsurface processes.

Today, fine spatial resolutions of large-scale hydrological models offer a unique opportunity to study expansion and contraction of GW discharge zones. In this study, beyond usual basin-scale estimates of groundwater contribution to river flow, we analyze the spatio-temporal distribution of groundwater discharge zones over several French regions. We use regional physically-based groundwater models from the Aquifer platform (Vergnes et al., 2020) covering part of France with simulation from 1958 to 2022. Aquifer models (Section 2) simulate the spatial distribution of the surface water and energy balances as well as the aquifer and river flows, including the river-aquifer interaction. To assess the spatial variability of GW discharge zones, we rely on two observation data sets (Sections 2.2.1 and 2.2.2). Then, we assess the temporal variability of GW discharge based on an observation network of river intermittence (Section 2.2.3). These two steps constitute an innovative approach to evaluate regional groundwater models from surface water observation. Note that Abhervé et al. (2024) recently used river intermittence to calibrate groundwater models at finer scale in crystalline aquifers (see also Mimeau et al., 2024, who used a combination of “process-oriented” and stochastic models to predict river intermittence). Such assessment gives insight on the dynamic and static biases of models, which should help identify where improvements of the groundwater parameters and inputs are the most needed. Methods and results are presented in Section 2 and 3, respectively, and discussed in Section 4 including perspectives and a focus on groundwater withdrawals impact.

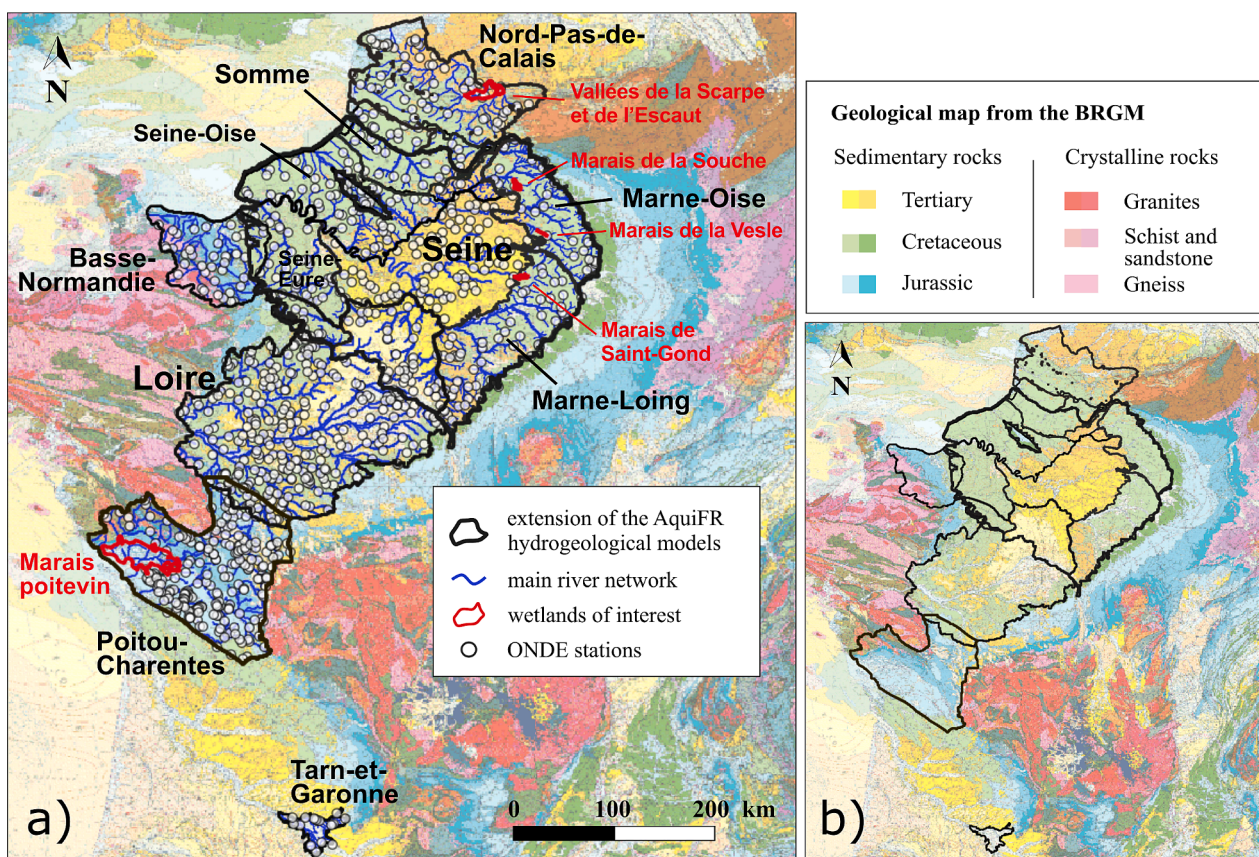


Fig. 1. a) Map of the spatially-distributed groundwater models within the Aquifer platform. Simulated rivers predefined in the models are illustrated by blue lines. White dots represent ONDE stations (French observation network of river intermittence). Red polygons delimit wetlands of interest. b) Geological units with a simplified legend (BRGM, 2008). (For interpretation of the references to color in this figure legend, the reader is referred to the web version of this article.)

2. Materials and methods

2.1. Hydrological models of the study area

2.1.1. Description of the AquiferFR modelling chain

The AquiferFR groundwater modelling platform covers around one-third of the French mainland area and half of the French aquifers (Fig. 1). AquiferFR aims at monitoring and providing seasonal forecasts of the groundwater as well as to project its long-term evolution in order to support decision-making at regional scale. It consists in a modelling chain gathering meteorological inputs (SAFRAN, Quintana-Seguí et al., 2008), a land surface model (SURFEX, Le Moigne et al., 2020; Masson et al., 2013) and regional groundwater models (Vergnes et al., 2020).

Within the modelling chain, the SURFEX land surface model simulates groundwater recharge and surface runoff. Then, hydrogeological models use these variables as inputs (Vergnes et al., 2020). SURFEX uses atmospheric variables provided by SAFRAN to solve the energy and water budgets at the land-atmosphere interface. While SURFEX relies on a grid resolution of 8 km, recharge, surface runoff and evapotranspiration are modelled within sub-grids (or tiles) representing different land cover fractions (Masson et al., 2013). A diffusion scheme is used to model the temperature and water transfer in the soil thanks to a “mixed” form of the Richards equation. Surface runoff is function of the fraction of the saturated area (Le Moigne et al., 2020). The SURFEX water balance can be summarized by Eq. (1):

$$\Delta\omega = P - AET - \text{Infiltration} - \text{Surface runoff} \quad (1)$$

where $\Delta\omega$ is the soil water storage variation, P precipitation and AET actual evapotranspiration.

A thorough evaluation of the simulated recharge was made using lysimeters (Sobaga et al., 2023a), and shows the sensitivity to the soil parameter profiles, which remains difficult to determine. Additionally, soil moisture and evapotranspiration simulated by SURFEX were evaluated at the French scale (Le Moigne et al., 2020). Although Vergnes et al. (2020) have included groundwater capillary rise within SURFEX, this possibility is not activated here, especially due to the fact hydrological models and SURFEX land surface models do not use the same spatial grids.

Within the platform, MARTHE (Thiéry, 2015) and EAUDYSSÉE (Saleh et al., 2013) simulate unsaturated zone transfer, groundwater flows, and groundwater-rivers exchanges over five and seven regions, respectively (Supplemental file 1). Each model is spatially distributed and solves a 2D diffusivity equation (Darcy law in combination with the conservation mass principle) in multi-layer aquifers. Vertical flow is estimated between the different aquifers based on conductance concept (Harbaugh, 2005) or with explicit simulation of aquitards. Groundwater withdrawals are included in the model based on incomplete reported values (Vergnes et al., 2020). Eq. (2) describes the groundwater flow equation and associated boundary conditions implemented in MARTHE and EAUDYSSÉE:

$$\text{div}\left(\overrightarrow{K\text{grad}H_{gw}}\right) + \text{Rech} - Q_{ex} - Q_{pump} = S \frac{\partial H_{gw}}{\partial t} \quad (2)$$

where $Q_{ex} = \max(T_p(H_{gw} - Z_{riv}), Q_{lim}, Q_{riv})$ refers to river-aquifer exchanges. Z_{riv} is the elevation of the river level, Q_{lim} a maximum infiltration flow from the river to the aquifer, Q_{riv} the flow in the river cell, and T_p a transfer coefficient linked to the riverbed characteristics. If there is no river defined in the cell, $Q_{riv} = Q_{lim} = 0$ and $Z_{riv} = Z_{topography}$. S is a storage coefficient, K hydraulic conductivity, H_{gw} the hydraulic head in the aquifer and Q_{pump} pumping rate. Infiltration from SURFEX is converted into groundwater recharge (Rech) through a linear unsaturated zone reservoir. Note that Eq. (1) and (2) are for grid cell of same size. Within Eq. (2), GW discharge corresponds to $Q_{ex} > 0$.

2.1.2. Representation of rivers in AquiferFR groundwater models

The finest spatial resolution of each regional application varies from 100 m to 1 km (Supplemental file 1). Within a regional model, finer resolution is used close to rivers for a better resolution of the aquifer-river exchange, and close to the watershed limits. Location of river is set based on a minimal drainage area, typically 10–50 km² (Fig. 1) depending on the model resolution (Vergnes et al., 2020). Therefore, the smallest rivers are not explicitly represented in models given that the actual minimum drainage area (i.e. the minimal area required to generate a stream) over the study area is close to 1 km² (Mardhel et al., 2021) (see the example for the Seine-Eure region in Supplemental file 2). These predefined rivers allow simulating river flow propagation and accurate river-groundwater exchanges based on simulated river water level. Thus, groundwater-river relationship is modeled as a fully coupled model in which river flow and water level are determined by upstream groundwater discharge.

As soon as the hydraulic head in groundwater is above the surface topography or above the water level in the predefined river network, groundwater feeds surface water bodies. Therefore, GW discharge, sometimes called “GW seepage” (Abhervé et al., 2023), here corresponds either to river baseflow, sources or aquifer overflow.

2.1.3. Groundwater model parametrization

Each regional model gathered in the AquiferFR platform was developed and calibrated independently, based on stakeholder requests. As the calibration was performed with another land surface model than SURFEX, their implementation within AquiferFR made it necessary to perform a new calibration (Vergnes et al., 2020).

Groundwater parameters (aquifers thickness, specific yield, hydraulic conductivity and their spatial variability) were first defined based on available local data (geological maps, geological logs, pumping tests). Calibration relied on groundwater levels and on river flows. The occurrence of groundwater discharge areas is sensitive to bias on the simulated groundwater levels (Abhervé et al., 2023; Vergnes and Habets, 2018). The AquiferFR platform was assessed by comparison of the simulation with observed piezometric levels and river flows in Vergnes et al. (2020) and this study is going further by assessing the area prone to aquifer overflow.

2.2. Observed surface hydrological data

2.2.1. River network maps

Simulated GW discharge zones are compared to the vectorial map of French rivers BD TOPO (Institut national de l’information géographique et forestière, 2022) that is derived from photometry and topography. It includes perennial and intermittent rivers, artificial rivers as well as canals, but excludes ditches.

2.2.2. Wetland maps

Simulated GW discharge zones are also compared to the main wetlands, those with a recognized interest and with clearly defined geographical boundaries. The international RAMSAR protected sites are exclusively wetlands (International convention on Wetlands (Ramsar), 1971). Some wetlands are also reckoned as Natura 2000 protected sites that stem from the European Birds and Habitats Directive (European Commission, 1992). Wetland maps are available on the National Inventory of Natural Heritage portal (Muséum national d’Histoire naturelle, 2022, 2023a). Among RAMSAR-Natura 2000 sites, we selected five wetlands corresponding to marshes large enough to be compared to the simulated GW discharge zones. These selected wetlands correspond to valleys with wet meadows or aggregation of ponds and channels (Fig. 1 and Table 1).

In addition, we use the potential wetlands map at a 5 m-resolution available from the National Inventory of Natural Heritage portal (Muséum national d’Histoire naturelle, 2023b). This map was obtained by Rapinel et al. (2023) applying a random forest model on topographic,

Table 1

Characteristics of RAMSAR and Natura 2000 wetlands selected for this study. Note that wetland areas slightly differ in this study compared to official protected areas.

Wetlands	Regional model	Short description	Area [km ²]
Vallées de la Scarpe et de l'Escaut (RAMSAR)	Nord-Pas-de-Calais	ponds, marshes, peatlands, streams, ditches, canals, marsh forests	275
Marais de la Souche (Natura 2000)	Marne-Oise	peatlands, marshes	43
Marais de la Vesle en amont de Reims (Natura 2000)	Marne-Oise	wet meadows, peatlands, marshes	8
Le Marais de Saint-Gond (Natura 2000)	Marne-Loing	wet meadows, peatlands, marshes	31
Marais Poitevin (Natura 2000)	Poitou-Charentes	wet meadows	1183

geological and river network maps and using 135,508 field plots (whose 39 % corresponds to wetlands) from the French archive databases.

2.2.3. River intermittence observations

The French observation network of river intermittence, ONDE (Office Français de la Biodiversité (OFB), 2022), monitors the occurrence of river flow since 2011 over 3417 river stations (Fig. 1) once a month during the low-flow season from May to September. Three river conditions can be reported based on a visual observation of the river: (1) the river is flowing, (2) there is water but the river is not flowing and (3) the river is dry. Such data are now used as drought indicators that help authorities to adapt water restriction to the drought situation.

AquiFR domain includes 1219 ONDE stations, dispatched regionally (Table 2). We selected stations i) whose upstream area, computed with a ~30 m-resolution DEM, is lower than 500 km² to focus on headwater but contains at least three AquiFR cells; ii) with at least 60 % of data over the 2012–2022 period; iii) where intermittence was observed at least once from 2012 to 2022. This leads to about 515 gauges. Of these, models estimate a contribution of the GW discharge in the upstream area for 396 stations. Only these last gauges are considered in this study (Table 2).

2.3. Methods for comparing simulated results and observed data

AquiFR runs from August 1958 to July 2022. Spatial distribution of simulated GW discharge is saved at a monthly time step. We first

Table 2

Number of ONDE river stations selected by successive criteria for each regional groundwater model within the AquiFR platform. The last criterion (last column) is relative to the model in the sense that the comparison between observed intermittence and simulated groundwater discharge is not possible at stations where the model does not produce any groundwater discharge.

Regions/sub-basins	Number of selected ONDE stations			
	within the model area	with an appropriate upstream area and enough observed data	with at least one observed intermittence	with groundwater discharge occurring at least once in the upstream area
Somme	31	31	14	11
Poitou-Charentes	232	172	131	108
Basse-Normandie	33	29	10	8
Nord-Pas-de-Calais	57	43	19	19
Tarn-et-Garonne	16	13	8	6
Somme	38	37	20	14
Loire	299	187	98	55
Seine	317	201	117	95
Seine-Eure	50	34	14	9
Seine-Oise	66	61	32	25
Marne-Oise	27	19	16	14
Marne-Loing	53	51	36	32

compare the spatial distribution of GW discharge zones with river network and wetland maps (Section 2.3.1 and Section 2.3.2). Then, we compare GW discharge dynamic with observations of river intermittence (Section 2.3.3) and assess the time variability of GW discharge within wetlands (Section 2.3.4).

2.3.1. Spatial distribution of rivers

We compare GW discharge location with the river network (BD TOPO). We expect that one part of GW discharge occurs along the rivers predefined within groundwater models (Section 2.1.2). In addition, we aim to compare the location of GW discharge zones with headwater streams not represented within groundwater models, in spite of their importance (Benstead and Leigh, 2012; Messenger et al., 2021). Some deviations are expected given that: i) the BD TOPO includes canals and artificial rivers. ii) all GW discharge zones are not prompt to generate rivers and could correspond to wetland or would not produce enough flow to generate a water course, or at least generate visible flow. Note that here, all simulated GW discharge zones are considered, without excluding meshes where the associated flow would be potentially too weak to feed surface water.

First, river network maps are rasterized on the same grid than each regional groundwater model (Supplemental file 1) in order to compare them with the simulated map of GW discharge zones. To do so, meshes of the rasterized river network are considered as rivers if they host at least one river from the vectorial BD TOPO map. Second, model meshes are considered as static GW discharge zones where GW discharge is simulated at least 50 % of the time during the last 30-year, from 1991 to 2021, in order to compare monthly model outputs with static observed river maps. This choice is motivated by the fact that observed river maps contain the main perennial and intermittent rivers. Therefore, stream sections fed by groundwater less than six months per year could be under-represented by the GW discharge static map. However, choosing a threshold at 25 and 75 % of the time does not change the main conclusions (Supplemental file 3).

The criterion (D) characterizes the overlap between GW discharge static map and observed rivers map. For each mesh, D relies on two criteria (D_{so} and D_{os}) (Abhervé et al., 2023) as described below:

- D is not attributed where there is no groundwater discharge neither observed rivers
- $D = 0$ where there is a groundwater discharge and an observed river
- $D = D_{so}$ where there is a groundwater discharge and no observed rivers
- $D = -D_{os}$ where there is an observed river and no groundwater discharge

where D_{50} is the distance to the closest observed river and D_{os} the distance to the closest simulated GW discharge zone. Thus, D corresponds to a distance between simulated GW discharge and observed rivers. D is optimal when close to zero, negative in meshes where observed rivers are not reproduced by the model, and positive where GW discharge zones are simulated without observed rivers. Negative and positive D values may be due to too low or too high groundwater levels, respectively.

2.3.2. Spatial distribution of wetlands

The comparison between the spatial distribution of GW discharge and RAMSAR-Natura 2000 wetlands location is performed visually and thanks to a criterion. Note that wetlands geometry was slightly simplified by grouping fragmented and tortuous wetland areas in order to compare easily modelled and observed maps. The criterion assesses the percentage of the wetland area covered by GW discharge zones. We also compute this same criterion but considering an extended wetland area in order to assess whether GW discharge zones occur outside the protected wetland area. This extended area is obtained by simply adding a buffer zone of 0.3–3 km (in function of the wetland size, i.e. $0.1 \times \sqrt{\text{wetland area}}$). The criterion is computed considering two extensions of the simulated GW discharge, based on the occurrence frequency: one and six months a year. Note there is no data related to time variations of surface water occurrence in wetlands. Therefore, we propose to evaluate if models simulate GW discharge at least once a year in wetlands, and whether these GW discharges are perennial at least six months a year.

In addition, we also compare visually GW discharge zones and RAMSAR-Natura 2000 wetlands location with the potential wetlands map (Rapinel et al., 2023). This second comparison allows identifying the potential presence of non-referenced wetlands (i.e. un-protected by RAMSAR or Natura 2000 conventions).

2.3.3. Spatio-temporal dynamics of river intermittence

Observed river intermittence at ONDE stations is compared with monthly flow produced by all GW discharge occurring in the upstream area of each station (m^3/month). ONDE data are simplified in two classes, cases with water in the river but without river flow are considered as a “dry river” condition. Because observations are boolean and available around six months a year during the dry season from 2012 to 2022, we compute three scores based on a contingency table (Eqs. (1)–(3)) for each station. The false-alarm rate (FAR) is the number of times a river dries up in the model while it is not the case actually (b), divided by the number of times a river dries up in the model. The missed-alarm rate (MAR) is the number of times a river dries up actually while it is not the case in the model (c), divided by the number of times the river dries up actually. The critical success index (CSI) is the number of times a river dries up both actually and in the model (a), divided by the sum of good, false and missed alarms. FAR and MAR have to be minimized while CSI has to be maximized.

$$FAR = b/(a + b) \quad (3)$$

$$MAR = c/(a + c) \quad (4)$$

$$CSI = a/(a + b + c) \quad (5)$$

We assume that river drying up can occur before GW discharge fully ceases in upstream areas of stations, especially since there might be some flows within the riverbed. Consistently, we define a GW discharge flow threshold below which we consider the river dries. This threshold is constant over the period 2012–2022. The value of this threshold is obtained by computing CSI scores for each simulated GW discharge flow value and keeping the value maximizing the CSI score. Not surprisingly, the thresholds are above $0 \text{ m}^3/\text{s}$ which is consistent with the persistence of a flow within the river bed even when the river is dry.

2.3.4. Spatio-temporal dynamics of wetlands

While there is currently no observation recording water quantity in wetlands, we propose to complete the spatial assessment (Section 2.3.2) by computing the time evolution of the flow produced by all GW discharge zones within each wetland. We focus on the evolution of this groundwater contribution at monthly scale from 1958 to 2022 as well as its average seasonal behavior.

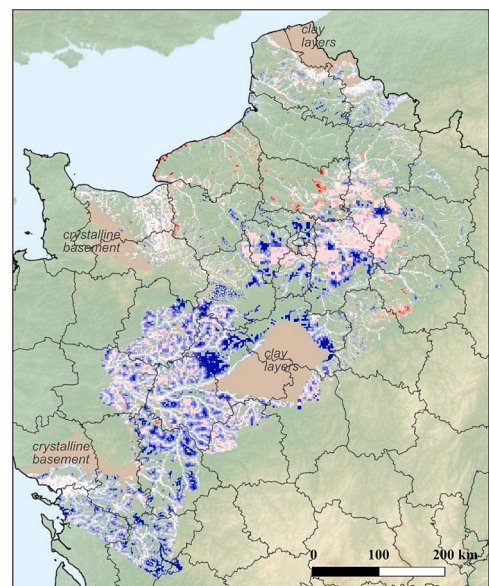
3. Results

3.1. Comparing rivers and wetlands location with static GW discharge map

3.1.1. River network comparison

Fig. 2 illustrates the spatial variation of criterion D over the study area. Maps of D for each region or sub-basin are provided in Supplemental file 4. As expected, most of the rivers which are predefined in groundwater models correspond to a D value of 0 (in white on Fig. 2) highlighting that groundwater supports them on most of the river section. Regarding headwater rivers, we find sparse small areas where GW discharge is simulated without observed rivers (in red on Fig. 2 corresponding to $D > 0$). The biggest area ($\sim 90 \text{ km}^2$) appears in Marne-Loing. Conversely, more areas present rivers but no GW discharge (in blue on Fig. 2 corresponding to $D < 0$) like in headwater rivers in Nord-Pas-de-Calais, in the South of Seine-Eure and in several parts of Poitou-Charentes. Tarn-et-Garonne and Loire models also show large areas with a negative D value (Supplemental file 4). Finally, patches ($\sim 1\text{--}10 \text{ km}^2$) with positive and negative discrepancies emerge locally in all regions.

Fig. 3 synthesizes the distribution of D with one histogram for each regional model. Median (η) and mean of absolute value (μ_{abs}) of D are



Distance [m] between observed rivers and simulated groundwater discharge zones (< 0 where simulated groundwater discharge is missing compared to observed rivers)

Fig. 2. Map of the criterion D representing the distance between observed rivers and simulated groundwater discharge zones at each model mesh. D is negative in meshes containing observed rivers but no groundwater discharge, and inversely. D is not attributed where there are neither observed rivers nor groundwater discharge. The color scale is limited here to -5000 and 5000 m (values range from around $-20,000$ to $+20,000 \text{ m}$). Areas with low-capacity aquifers are excluded from this study (light brown color). (For interpretation of the references to color in this figure legend, the reader is referred to the web version of this article.)

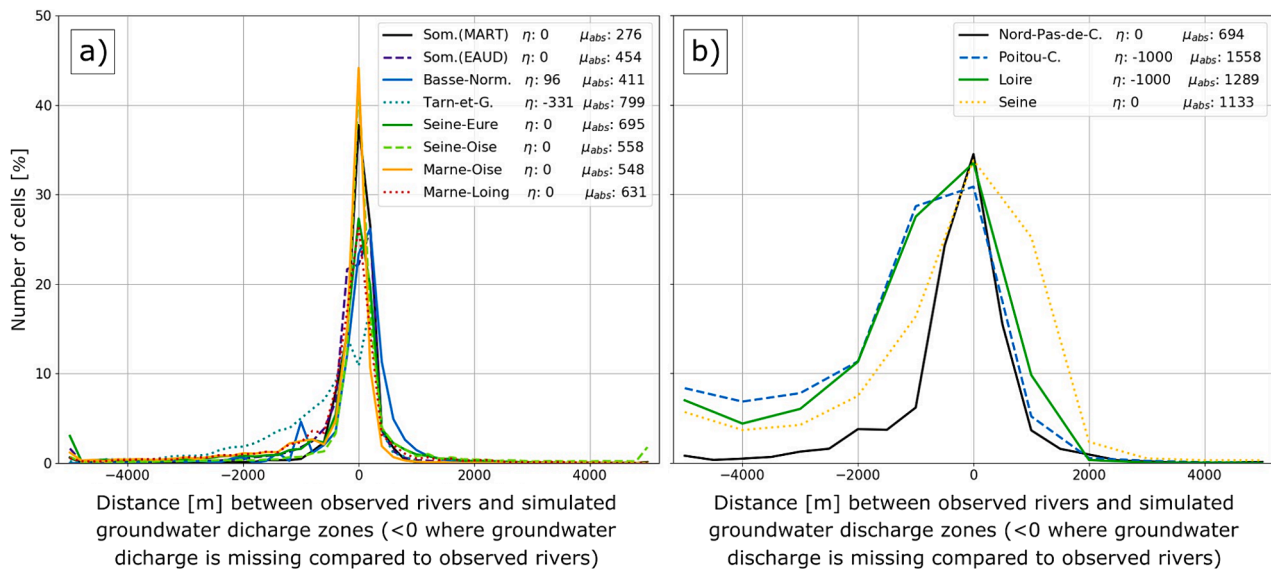


Fig. 3. Histogram of the criterion D , representing the distance [m] between observed rivers and simulated groundwater discharge for each region. a) Regional models with the finest spatial resolution (≤ 250 m). b) Regional models with the biggest spatial resolution (≥ 500 m). D is negative in meshes containing observed rivers but no groundwater discharge and inversely. For a better visualization, distances higher (lower) than 5000 m (resp. -5000 m) are here considered equal to 5000 m (resp. -5000 m). Values extend to $\pm 10,000$ and $\pm 20,000$ m for regional models with the finest and the biggest spatial resolution, respectively. Median value (η) and mean of absolute values (μ_{abs}) are given in meters in the legend.

given in the legend of Fig. 3. On average, histograms confirm that GW discharge static map and river network overlap. Indeed, η is very close to 0 m for all regions except Poitou-Charentes ($\eta \sim -1000$ m), Loire ($\eta \sim -1000$ m) and Tarn-et-Garonne ($\eta \sim -331$ m). For these three regions, histograms highlight that groundwater levels could be preferentially underestimated in a significant fraction of the modelled area. While biases at regional scale are relatively low ($\eta \sim 0$ m), μ_{abs} values highlight the presence of smaller areas with either positive or negative D values for all regions ($\mu_{abs} = 276\text{--}1558$ m) with worst values for Poitou-Charentes, Loire and Seine regions ($\mu_{abs} = 1135\text{--}1558$ m). Note that Poitou-Charentes, Loire and Seine groundwater models have the biggest area and the coarsest spatial resolution (≥ 1000 m) (Fig. 3b). For these regional models, the actual distribution of GW discharge zones can not be fully captured where river density is finer than model resolution.

3.1.2. Wetlands location comparison

Simulated GW discharge zones (in blue on Fig. 4) cover at least once a year almost all the Poitevin marsh (90 %) and most of the Scarpe-Escaut, Vesle and Souche wetland areas (~ 70 %, Supplemental file 5 **Erreur! Source du renvoi introuvable.**). Simulated GW discharge zones cover only 49 % the Saint-Gond wetland, along the main river and some downstream cells (lower-right panel on Fig. 4). Wetland area covered by GW discharge zones decreases of ~ 20 % when considering GW discharge occurring at least six months a year except in the Saint-Gond wetland where it drops by 41 % (Supplemental file 5).

In general, the comparison between simulated GW discharge zones and potential wetland maps (Supplemental file 7 Fig. 4) is consistent with the river network comparison (Section 3.1.1). This is explained by the fact that most of the potential wetlands are located around rivers. In addition, potential wetlands cover almost all the RAMSAR-Natura 2000 wetland areas (Supplemental file 7). Finally, this visual comparison also highlights numerous potential wetlands within flat areas covered by clay layers like in Nord-Pas-de-Calais (upper-right panel on Fig. 4) and Loire (Supplemental file 7) models and within areas covered by crystalline bedrock like in Poitou-Charentes (lower-left panel on Fig. 4) and Basse-Normandie (Supplemental file 7) models.

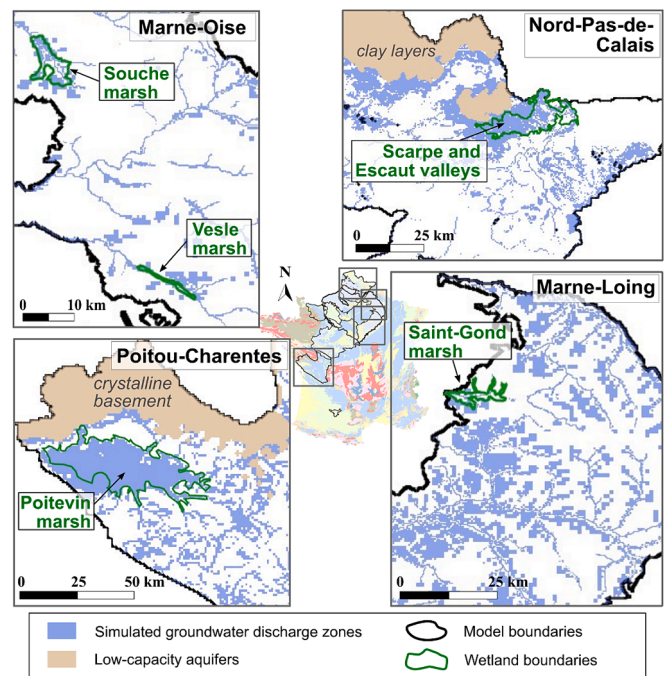


Fig. 4. Comparison between simulated groundwater discharge zones (blue) and RAMSAR-Natura 2000 wetlands (green) location. Areas with low-capacity surface aquifers are excluded from this study (light brown color). (For interpretation of the references to color in this figure legend, the reader is referred to the web version of this article.)

3.2. GW discharge temporal variability in rivers and wetlands

3.2.1. Comparing simulated GW discharge with river intermittence observations

The comparison between GW discharge and river intermittence observations is illustrated on Fig. 5 at four stations corresponding to stations with the best and average score for Marne-Loing and Poitou-

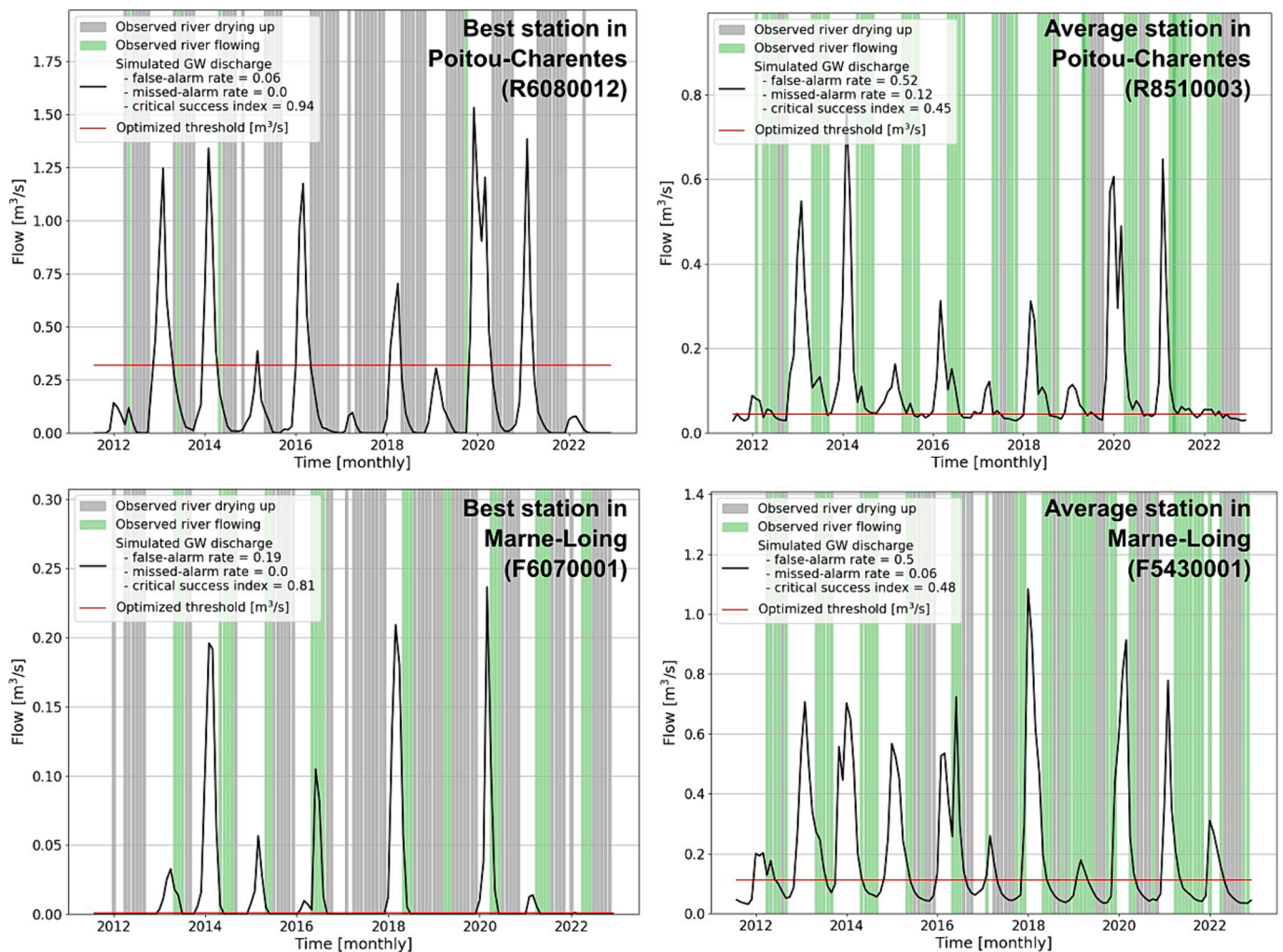


Fig. 5. Comparison between simulated groundwater discharge flow in upstream area of ONDE stations (black line) and observed river intermittence (gray/green vertical lines) in Poitou-Charentes (first row) and Marne-Loing (second row) models. Left column: stations showing the best score. Right column: stations showing the average score. The horizontal red line represents the GW discharge flow threshold that optimizes the CSI score. Below this threshold, the river is considered dry. (For interpretation of the references to color in this figure legend, the reader is referred to the web version of this article.)

Charentes regions. Similar figures are available for all regions in [Supplemental file 8](#). Overall, rivers can run dry although GW discharge does not fully ceased in models. Over the 396 selected stations, groundwater model continues to feed surface water upstream of the station for $\sim 75\%$ of observed river drying up events. The optimized threshold (symbolized by a red line on [Fig. 5](#)), below which we consider that rivers run dry, leads to both false-alarms (like in 2013 and 2014 at station F5430001 in Marne-Loing) and missed-alarms (like in 2020 at station F8510003 in Poitou-Charentes).

As explained in [Section 2.3.3](#), the GW discharge flow threshold (in red on [Fig. 5](#)) was defined to maximize the CSI score. For each ONDE station, we obtain a threshold value, associated with CSI, FAR and MAR scores. Optimized threshold values (m^3/s) are consistent with the upstream area of each station (**Erreur! Source du renvoi introuvable.**). Noteworthy, the threshold variability is important ($0\text{--}0.2 \text{ m}^3/\text{s}$ for basins of $\sim 30 \text{ km}^2$).

[Fig. 6](#) presents the distribution of FAR, MAR and CSI scores for each regional model. Median CSI varies from ~ 0.2 (worst value for Tarn-et-Garonne model) to 0.5 (best value for Marne-Oise model). Median MAR score is low (~ 0.2) for all models, meaning that in average models miss only few river drying events (assuming here that simulated rivers are dry when the GW discharge flow falls below the threshold value). However, FAR scores are relatively high (median ~ 0.6), meaning that a

large number of alarms are false. Worst results are obtained in Tarn-et-Garonne, Basse-Normandie and Somme models, especially regarding FAR score. Best results are obtained in Poitou-Charentes, Nord-Pas-de-Calais and Marne-Oise models. Results are contrasted as a large number of stations exhibit poor scores but around 30% of stations have FAR and MAR scores below 0.5 with a CSI score above 0.5 . Potential improvements and limits of this comparison such as score choice or river withdrawals impact are discussed in [Section 4](#).

3.2.2. Groundwater discharge temporal variability in wetlands

Seasonal variations of the GW discharge flow illustrate the importance of groundwater contributions to wetlands, which buffer climate seasonality ([Fig. 7](#)). During dry season, the total groundwater contribution ranges from ~ 5 to 60 mm/month for the Poitevin and Vesle ([Supplemental file 9](#)) marshes, respectively. The annual average value of simulated GW discharge flow in wetlands ranges from ~ 200 to 1000 mm/yr and exceeds effective rainfall occurring within wetlands, especially during dry season ($\sim \text{May--October}$). On an annual scale, the ratio of GW discharge flow on recharge rate ranges from ~ 1.2 to 3.7 for Saint-Gond and Vesle marshes, respectively. Therefore, wetlands are largely supported by rainfall infiltrated outside of their surface boundaries.

At inter-annual scale, the groundwater contribution during dry season appears relatively stable in the Poitevin marsh and in the Scarpe-

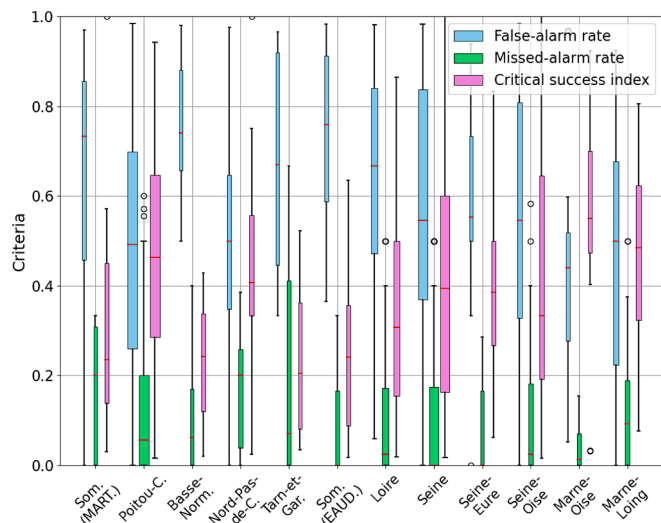


Fig. 6. Distribution of false- and missed-alarm rates and critical success index for each region. False- and missed-alarm rates equal to 0 and a critical success index equal to 1 indicate a perfect forecast. Upper (lower) box boundary represents 75th (resp. 25th) percentile, red line the median value, and whiskers the 75th (resp. 25th) percentile plus (resp. less) 1.5 times the interquartile range. Box width depends on the number of ONDE stations for each region (108 and 6 stations for Seine and Tarn-et-Garonne, respectively). (For interpretation of the references to color in this figure legend, the reader is referred to the web version of this article.)

Escaut valleys and more variable in Saint-Gond (ranging from 5 to 15 mm/month), Vesle (from 10 to 100 mm/month) and Souche (from 30 to 60 mm/month) wetlands (Supplemental file 9). This bigger variability during dry season is explained by the legacy of wet or dry pluri-annual periods in Marne-Loing and Marne-Oise aquifer models.

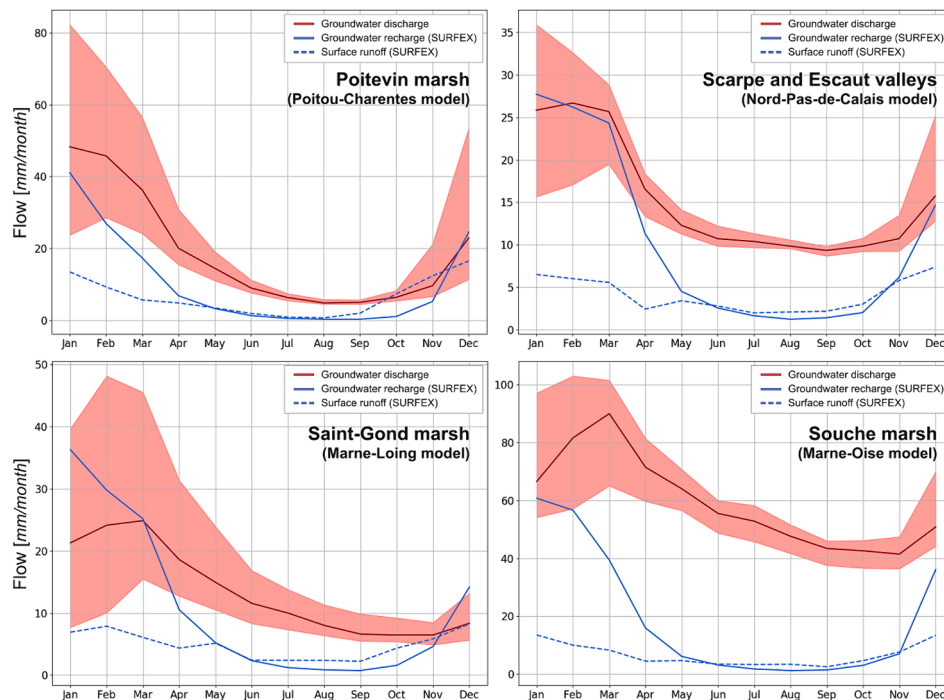


Fig. 7. Average seasonal variations (mm/month) of simulated groundwater contribution (red), recharge (blue) and surface runoff (dashed blue) within RAMSAR-Natura 2000 wetlands. Shaded areas represent the 25th and 75th annual percentiles for the groundwater contribution across the 1991–2021 period. (For interpretation of the references to color in this figure legend, the reader is referred to the web version of this article.)

4. Discussion

4.1. On the difficulty to compare GW discharge and surface water location

Overall, GW discharge location matches with the presence of wetlands and rivers (Figs. 2 and 4) while wetlands and most of headwater streams are not predefined in groundwater models. Results regarding river comparison were expected as studied regions are not mountainous and not subject to arid climate so that rivers highly depend on water table rather than on upstream flow (Costigan et al., 2016; Shanfield et al., 2021) especially in headwater basins. Therefore, results would slightly differ in other regions owing to climate, geology or geomorphology (Konrad, 2006). Here, only a few river sections do not match with GW discharge zones. In this case, rivers could potentially seep into underlying aquifers (Jasechko et al., 2021; Sanz et al., 2011; Thierion et al., 2012; Vergnes and Habets, 2018). Regarding wetlands, lateral surface water inputs and surface water retention are not taken into account in our approach. We only focus on GW discharge occurring within protected wetland boundaries, thus excluding those occurring farther away within the hydrogeologic watershed which can extend beyond the topographic watershed (Huggins et al., 2023).

Headwater basins lack of monitoring wells and river stations. Studying deeper these areas and the reasons of mismatch between surface water observation and simulated groundwater levels would help to improve hydrological models. For example, many rivers in Tarn-et-Garonne, Loire and Poitou-Charentes (in blue on Fig. 2) are located in areas where there is no simulated GW discharge. Several explanations are possible such as: (1) the role of thin alluvial aquifers or clay layers not taken into account within regional models, (2) misrepresentation of confined (resp. unconfined) behavior disconnecting (resp. connecting) aquifers and surface water, (3) incomplete representation of human impacts (artificial rivers, withdrawals) or (4) imperfect model calibration.

The surface-groundwater comparison is difficult when focusing on small rivers or wetlands because the variability of the groundwater

contribution to surface water increases at small scale (Krakauer et al., 2014; Schaller and Fan, 2009). Regional groundwater models calibration relies on local parameter estimates, groundwater levels recorded in sparse monitoring well networks and on river discharge stations. This calibration fails to fully capture hydraulic conductivity variability, which is highly heterogeneous and ranging over several order of magnitude, and controls groundwater levels (Abhervé et al., 2023).

RAMSAR-Natura 2000 wetlands appear also in low-capacity aquifers not studied here (either crystalline aquifers or clay layers overlying aquifers), such as the “Sologne wetlands” in Loire regional model, the “Audomarois marsh” in Nord-Pas-de-Calais, the “Druance Basin” and the “Upper Orne Valley” in Basse-Normandie (Supplemental file 7). Similarly, potential wetlands are identified in Poitou-Charentes and Nord-Pas-de-Calais (in red on Fig. 4) in areas hosting low-capacity aquifers while these areas are not known to host protected wetlands but rather a very dense river network. Groundwater models implemented within the Aquifer platform focus on hydraulic heads within aquifer layers and do not represent low-capacity aquifers. Reproducing the spatial distribution of GW discharge in these sub-regions would require improving low-capacity aquifers representation and spatial resolution (including natural and agricultural drainage networks). In addition, the wetland inventory is incomplete, so that simulated GW discharge zones could correspond to unclassified wetlands. Therefore, we identify some of these areas based on a national inventory (Office Français de la Biodiversité (OFB), 2024) currently in progress (Supplemental file 10). However, most wetlands are located along rivers making it difficult to separate groundwater contribution to rivers and wetlands within regional models.

Finally, the spatial scale and the associated resolution of regional groundwater models limit the comparison with surface water location (Fig. 3). In addition, model resolution impacts calibration and resulting groundwater levels (Guillaumot et al., 2022), as well as surface-groundwater interaction (Vergnes and Habets, 2018). Therefore, the location of GW discharge zones and their dynamics should be interpreted carefully especially when focusing on local scale even if we show that, at first order, GW discharge zones match with surface water location and vice versa.

4.2. Implications of anthropogenic disturbances in hydrological dynamics

Human withdrawals representation appears essential to study groundwater-surface interaction (Guillaumot et al., 2022). Within the Aquifer platform, pumping rates vary seasonally but are similar each year. Taking into account groundwater withdrawals inter-annual variability (currently, inter-annual variations are only considered from ~1995 to ~2010 for half of the models), as well as adding surface water withdrawals, would be interesting to assess accurately their impact and could improve results regarding river intermittence (Datry et al., 2023). Indeed, while simulated groundwater withdrawals are relatively low at regional and annual scales (from 3 to 16 % of annual recharge), their influence on GW discharge could be more pronounced locally or during dry years as the highest annual ratio between pumping and recharge ranges from 13 % in Basse-Normandie and Marne-Oise to ~40 % in other regions (until 144 % in Tarn-et-Garonne).

In order to evaluate groundwater pumping impact on GW discharge and especially on protected wetlands and rivers followed by ONDE stations (Huggins et al., 2023; Zipper et al., 2024), we run models removing pumping from 2009 to 2022. We then evaluate the impact on groundwater contribution in August as illustrated by Fig. 8 focusing on the Poitou-Charentes region (see Supplemental file 11 for other regions). The impact, expressed in percentage on Fig. 8, corresponds to the difference between the average of GW discharge across 2011–2022 when withdrawals are considered and when they are removed. Groundwater contribution decreases when withdrawals are activated. A significant part of rivers and the outer limit of the Poitevin marsh appear strongly impacted by withdrawals. This confirms the need to improve pumping

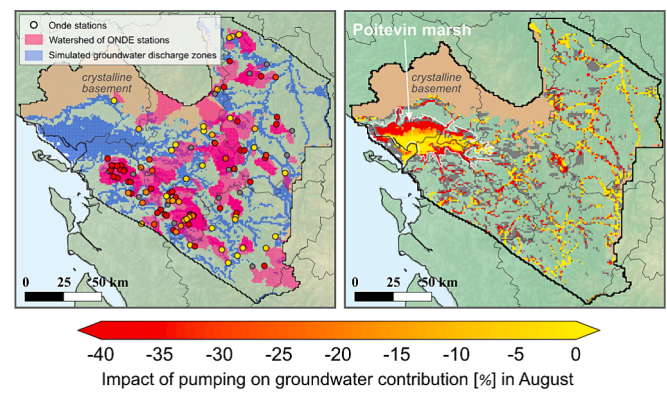


Fig. 8. Impact of pumping on groundwater contribution to surface water in August in Poitou-Charentes region, expressed as the difference between groundwater discharge without and with pumping (%). Left panel: impact at river ONDE stations; shaded pink and blue areas correspond to station upstream areas and to grid cells where groundwater discharge is simulated, respectively. Right panel: impact on all simulated groundwater discharge zones, including the Poitevin Marsh (white boundaries). Note the red-to-yellow scale is similar for the two panels and the minimum value is limited here to -40% for a better visualization. (For interpretation of the references to color in this figure legend, the reader is referred to the web version of this article.)

representation and associated impact on rivers (Condon and Maxwell, 2019; de Graaf et al., 2019; Jasechko et al., 2021; Sanz et al., 2011). In the same time, including river losses due to infiltration appears also essential but would require modeling more rivers in headwater basins.

4.3. Opportunity and challenges in linking river intermittence and groundwater

The total GW discharge flow in the upstream area of each ONDE station is used as a proxy of river drying up allowing comparing groundwater models with observed river intermittence. After all, results appear reliable for an important number of stations. For example, Fig. 9 shows the value of the optimized threshold (below which we can infer that rivers run dry) for two regions. The size of the circle representing stations is proportional to the CSI scores so that the more reliable stations have the biggest circles.

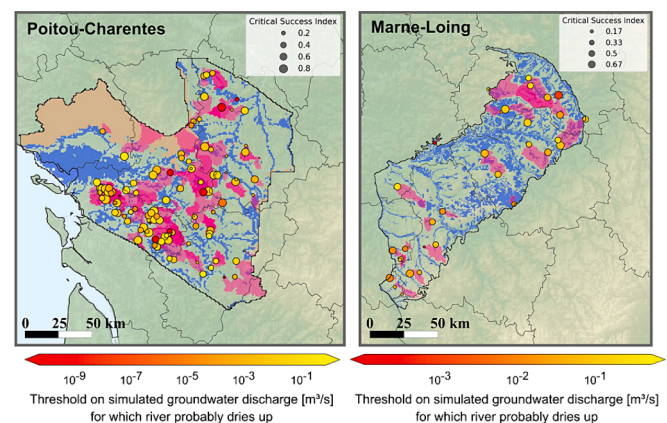


Fig. 9. Value of the optimized threshold, i.e. the groundwater discharge flow below which river probably dries up, for each ONDE stations in Poitou-Charentes and Marne-Loing regions (red-to-yellow colors in circles). Note the different color scales between the two regions. This approach is more reliable at stations where the critical success index is high (size of the circle). Shaded pink areas correspond to station upstream areas. Shaded blue areas correspond to grid cells where groundwater discharge is simulated on average. (For interpretation of the references to color in this figure legend, the reader is referred to the web version of this article.)

This preliminary study still needs improvements in order to be integrated within an operational chain to support decision making. Once again, there is no consideration of surface water routing processes in most of rivers in upstream areas of ONDE stations such as water retention, evaporation or infiltration. More studies are necessary in order to infer surface, soil and groundwater models weaknesses leading to discrepancies between GW discharge time-variations and observed river intermittence (Kirchner et al., 2023). The optimized threshold could be defined at monthly scale instead of a constant value and could be impacted by surface runoff and by other factors such as the basin area and the distance between GW discharge and the river station. All these factors could be integrated by predefining more rivers within regional models, as mentioned previously. As also mentioned in Section 4.2, improving groundwater withdrawal representation and including surface water withdrawal could be essential. The study of intermittence would also benefit from an improvement of the time scale from monthly to daily.

While wetlands are simply not implemented within groundwater models, upward flow between groundwater and soil could be implemented with SURFEX (Colin et al., 2023; Vergnes et al., 2014). Groundwater contribution to wetlands could be validated using remote sensing data to retrieve soil humidity or punctual observations of surface water occurrence in wetlands.

5. Conclusions

Regional scale groundwater models are difficult to calibrate and evaluate. Reproducing water table depth variability still appears as a major challenge for continental-scale hydrological models (Maxwell et al., 2015; Naz et al., 2023). In the same time, remote sensing datasets offer new opportunities to evaluate models and infer hydraulic parameters. They require to model in an integrated way surface water, soil and groundwater. Here, we compare for the first time at regional scale groundwater models and surface water occurrence, as suggested by Gleeson et al. (2021). As well as Abhervé et al. (2023, 2024), we show that data relative to surface water occurrence can be an additional information to sparse groundwater level observations.

Simulated GW discharge zones are more consistent with the observed location of rivers and wetlands when resolution is fine. In addition, GW discharge is well correlated with observed river. We infer that the smallest headwater rivers, generally more susceptible to intermittence, are blurred by the coarse spatial resolution of some groundwater models. We also highlight the importance of groundwater withdrawals on rivers during dry season. Further studies better considering withdrawals and modelling more headwater streams would be necessary in order to precise results and evaluate surface water resilience to droughts and human impact. This study opens the door to river and wetland drought forecasts using the AquifR platform.

CRedit authorship contribution statement

Luca Guillaumot: Writing – review & editing, Writing – original draft, Visualization, Resources, Methodology, Formal analysis, Data curation, Conceptualization. **Simon Munier:** Writing – review & editing, Software, Methodology, Conceptualization. **Ronan Abhervé:** Writing – review & editing, Methodology, Conceptualization. **Jean-Pierre Vergnes:** Writing – review & editing, Software. **Alexis Jeantet:** Writing – review & editing. **Patrick Le Moigne:** Writing – review & editing. **Florence Habets:** Writing – review & editing, Software, Project administration, Methodology, Conceptualization.

Declaration of competing interest

The authors declare that they have no known competing financial interests or personal relationships that could have appeared to influence the work reported in this paper.

Data availability

Shape files of the French river network are available at <https://geoservices.ign.fr/bdtopo> (last access: 24 January 2023). Observations of rivers intermittence through the ONDE network are available at <https://onde.eaufrance.fr/> (last access: 23 January 2023). Protected RAMSAR and Natura 2000 wetland boundaries are available at <https://inpn.mnhn.fr/telechargement/cartes-et-information-geographique/ep/ramsar> (last access: 8 September 2023) and <https://inpn.mnhn.fr/telechargement/cartes-et-information-geographique/nat/natura> (last access: 8 September 2023), respectively. The SURFEX source code is available at <http://www.umr-cnrm.fr/surfex/> (last access: 28 September 2023). The EAUDYSSÉE source code is available upon e-mail request to florence.habets@ens.fr. Questions about the MARTHE source code can be requested to marthe@brgm.fr. The SURFEX files are available upon e-mail request to patrick.lemoigne@meteo.fr. Output files and details about the AquifR code can be gathered upon e-mail request to simon.munier@meteo.fr.

Acknowledgments

This research was conducted within the AquifR framework (<https://www.geosciences.ens.fr/recherche/projets/aqui-fr>, last access: 28 September 2023) funded by the Office Français de la Biodiversité (OFB), France. Authors thank the different people contributing to the AquifR project at the French geological survey (BRGM), CNRS, ENS, Météo-France, CNRM, Mines ParisTech and Geosciences Rennes (France), and Claire Magand (OFB).

Appendix A. Supplementary data

Supplementary data to this article can be found online at <https://doi.org/10.1016/j.jhydrol.2024.132019>.

References

- Abhervé, R., Roques, C., Gauvain, A., Longuevergne, L., Louaisil, S., 2023. Calibration of groundwater seepage against the spatial distribution of the stream network to assess catchment-scale hydraulic properties. *Hydrol. Earth Syst. Sci.* 27, 3221–3239. <https://doi.org/10.5194/hess-27-3221-2023>.
- Abhervé, R., Roques, C., de Dreuzay, J.R., Detry, T., Brunner, P., Longuevergne, L., Aquilina, L., 2024. Improving calibration of groundwater flow models using headwater streamflow intermittence. *Hydrol. Process.* 38, 1–19. <https://doi.org/10.1002/hyp.15167>.
- Armandine Les Landes, A., Aquilina, L., De Ridder, J., Longuevergne, L., Pagé, C., Goderniaux, P., 2014. Investigating the respective impacts of groundwater exploitation and climate change on wetland extension over 150 years. *J. Hydrol.* <https://doi.org/10.1016/j.jhydrol.2013.11.039>.
- Barclay, J.R., Starn, J.J., Briggs, M.A., Helton, A.M., 2020. Improved prediction of management-relevant groundwater discharge characteristics throughout river networks. *Water Resour. Res.* 56, e2020WR028027. <https://doi.org/10.1029/2020WR028027>.
- Batelaan, O., De Smedt, F., Triest, L., 2003. Regional groundwater discharge: phreatophyte mapping, groundwater modelling and impact analysis of land-use change. *J. Hydrol.* 275, 86–108. [https://doi.org/10.1016/S0022-1694\(03\)00018-0](https://doi.org/10.1016/S0022-1694(03)00018-0).
- Baulon, L., Allier, D., Massei, N., Fournier, M., Bault, V., 2022. Influence of low-frequency variability on groundwater level trends. *J. Hydrol.* 606. <https://doi.org/10.1016/j.jhydrol.2022.127436>.
- Benstead, J.P., Leigh, D.S., 2012. An expanded role for river networks. *Nat. Geosci.* 5, 678–679. <https://doi.org/10.1038/ngeo1593>.
- Blazkova, S., Beven, K.J., Kulasova, A., 2002. On constraining TOPMODEL hydrograph simulations using partial saturated area information. *Hydrol. Process.* 16, 441–458. <https://doi.org/10.1002/hyp.331>.
- Blöschl, G., Bierkens, M.F.P., Chambel, A., Cudenneq, C., Destouni, G., Fiori, A., Kirchner, J.W., McDonnell, J.J., Savenije, H.H.G., Sivapalan, M., Stumpff, C., Toth, E., Volpi, E., Carr, G., 2019. Twenty-three unsolved problems in hydrology (UPH) – a community perspective. *Hydrol. Sci. J.* 64, 1141–1158. <https://doi.org/10.1080/02626667.2019.1620507>.
- Boé, J., Habets, F., 2014. Multi-decadal river flow variations in France. *Hydrol. Earth Syst. Sci.* 18, 691–708. <https://doi.org/10.5194/hess-18-691-2014>.
- Bouwer, H., Maddock, T.I., 1997. Making sense of the interactions between groundwater and streamflow: lessons for water masters and adjudicators. *Rivers*.
- Bresciani, E., Goderniaux, P., Batelaan, O., 2016. Hydrogeological controls of water table – land surface interactions. *Geophys. Res. Lett.* 1–9. <https://doi.org/10.1002/2016GL070618>.

- BRGM, 2008. Carte lithologique simplifiée [WWW Document]. géocatalogue. URL: <https://www.geocatalogue.fr/Detail.do?fileIdentifier=697c5ec0-7371-11dd-a5f6-005056b2266a> (accessed 1.22.24).
- BRGM, 2022. BDLISAV3 (Base de Données des Limites des Systèmes Aquifères) [WWW Document]. URL: <https://bdlisa.eaufrance.fr/> (accessed 6.13.23).
- Busch, M.H., Costigan, K.H., Fritz, K.M., Datry, T., Krabbenhoft, C.A., Hammond, J.C., Zimmer, M., Olden, J.D., Burrows, R.M., Dodds, W.K., Boersma, K.S., Shanfield, M., Kampf, S.K., Mims, M.C., Bogan, M.T., Ward, A.S., Perez Rocha, M., Godsey, S., Allen, G.H., Blaszcak, J.R., Jones, C.N., Allen, D.C., 2020. What's in a name? Patterns, trends, and suggestions for defining non-perennial rivers and streams. *Water* 12, 1980. <https://doi.org/10.3390/w12071980>.
- Colin, J., Decharme, B., Cattiaux, J., Saint-Martin, D., 2023. Groundwater feedbacks on climate change in the CNRM global climate model. *J. Clim.* 36, 7599–7617. <https://doi.org/10.1175/JCLI-D-22-0767.1>.
- Condon, L.E., Maxwell, R.M., 2019. Simulating the sensitivity of evapotranspiration and streamflow to large-scale groundwater depletion. *Sci. Adv.* 5. <https://doi.org/10.1126/sciadv.aav4574>.
- Cornette, N., Roques, C., Boisson, A., Courtois, Q., Marçais, J., Launay, J., Pajot, G., Habets, F., Cornette, N., Roques, C., Boisson, A., Courtois, Q., Marçais, J., 2022. Hillslope-scale exploration of the relative contribution of base flow, seepage flow and overland flow to streamflow dynamics. *J. Hydrol.* 610, 127992. <https://doi.org/10.1016/j.jhydrol.2022.127992>.
- Costigan, K.H., Jaeger, K.L., Goss, C.W., Fritz, K.M., Goebel, P.C., 2016. Understanding controls on flow permanence in intermittent rivers to aid ecological research: integrating meteorology, geology and land cover. *Ecology* 9, 1141–1153. <https://doi.org/10.1002/eco.1712>.
- Cuthbert, M.O., Gleeson, T., Moosdorf, N., Befus, K.M., Schneider, A., Hartmann, J., Lehner, B., 2019. Global patterns and dynamics of climate-groundwater interactions. *Nat. Clim. Chang.* 9, 137–141. <https://doi.org/10.1038/s41558-018-0386-4>.
- Datry, T., Larned, S.T., Tockner, K., 2014. Intermittent rivers: a challenge for freshwater ecology. *Bioscience* 64, 229–235. <https://doi.org/10.1093/biosci/bit027>.
- Datry, T., Truchy, A., Olden, J.D., Busch, M.H., Stubbington, R., Dodds, W.K., Zipper, S., Yu, S., Messenger, M.L., Tonkin, J.D., Kaiser, K.E., Hammond, J.C., Moody, E.K., Burrows, R.M., Sarremejane, R., Delvecchia, A.G., Fork, M.L., Little, C.J., Walker, R.H., Walters, A.W., Allen, D., 2023. Causes, responses, and implications of anthropogenic versus natural flow intermittence in river networks. *Bioscience* 73, 9–22. <https://doi.org/10.1093/biosci/biac098>.
- de Graaf, I.E.M., Gleeson, T., (Rens) van Beek, L.P.H., Sutanudjaja, E.H., Bierkens, M.F.P., 2019. Environmental flow limits to global groundwater pumping. *Nature* 574, 90–94. <https://doi.org/10.1038/s41586-019-1594-4>.
- Enemark, T., Peeters, L.J.M., Mallants, D., Batelaan, O., 2018. Hydrogeological conceptual model building and testing: a review. *J. Hydrol.* 569, 310–329. <https://doi.org/10.1016/j.jhydrol.2018.12.007>.
- European Commission, 1992. The Natura 2000 network of protected areas [WWW Document]. URL: <https://ec.europa.eu/environment/nature/natura2000/> (accessed 9.13.23).
- Fan, Y., 2015. Groundwater in the Earth's critical zone: relevance to large-scale patterns and processes. *Water Resour. Res.* 51, 3052–3069. <https://doi.org/10.1002/2015WR017037>.
- Fovet, O., Belemtoûri, A., Boithias, L., Braud, I., Charlier, J.B., Cottet, M., Daudin, K., Dramais, G., Ducharme, A., Folton, N., Grippa, M., Hector, B., Kuppel, S., Le Coz, J., Legal, L., Martin, P., Moatar, F., Molénat, J., Probst, A., Riotte, J., Vidal, J.P., Vinatier, F., Datry, T., 2021. Intermittent rivers and ephemeral streams: perspectives for critical zone science and research on socio-ecosystems. *Wiley Interdiscip. Rev. Water* 8, 1–33. <https://doi.org/10.1002/wat2.1523>.
- Franks, S.W., Gineste, P., Beven, K.J., Merot, P., 1998. On constraining the predictions of a distributed model: the incorporation of fuzzy estimates of saturated areas into the calibration process. *Water Resour. Res.* 34, 787–797. <https://doi.org/10.1029/97WR03041>.
- Gleeson, T., Wagener, T., Döll, P., Zipper, S.C., West, C., Wada, Y., Taylor, R., Scanlon, B., Rosolem, R., Rahman, S., Oshinlaja, N., Maxwell, R., Lo, M.H., Kim, H., Hill, M., Hartmann, A., Fogg, G., Famiglietti, J.S., Ducharme, A., De Graaf, I., Cuthbert, M., Condon, L., Bresciani, E., Bierkens, M.F.P., 2021. GMD perspective: the quest to improve the evaluation of groundwater representation in continental-to global-scale models. *Geosci. Model Dev.* 14, 7545–7571. <https://doi.org/10.5194/gmd-14-7545-2021>.
- Godsey, S.E., Kirchner, J.W., 2014. Dynamic, discontinuous stream networks: hydrologically driven variations in active drainage density, flowing channels and stream order. *Hydrol. Process.* 28, 5791–5803. <https://doi.org/10.1002/hyp.10310>.
- Grabs, T., Seibert, J., Bishop, K., Laudon, H., 2009. Modeling spatial patterns of saturated areas: a comparison of the topographic wetness index and a dynamic distributed model. *J. Hydrol.* 373, 15–23. <https://doi.org/10.1016/j.jhydrol.2009.03.031>.
- Guillaumot, L., Smilovic, M., Burek, P., De Bruijn, J., Greve, P., Kahil, T., Wada, Y., 2022. Coupling a large-scale hydrological model (CWatM v1.1) with a high-resolution groundwater flow model (MODFLOW 6) to assess the impact of irrigation at regional scale. *Geosci. Model Dev.* 15, 7099–7120. <https://doi.org/10.5194/gmd-15-7099-2022>.
- Güntner, A., Seibert, J., Uhlenbrook, S., 2004. Modeling spatial patterns of saturated areas: an evaluation of different terrain indices. *Water Resour. Res.* 40, 1–19. <https://doi.org/10.1029/2003WR002864>.
- Haas, J.C., Birk, S., 2019. Trends in Austrian groundwater – climate or human impact? *J. Hydrol. Reg. Stud.* 22. <https://doi.org/10.1016/j.ejrh.2019.100597>.
- Habets, F., Boé, J., Déqué, M., Ducharme, A., Gascoin, S., Hachour, A., Martin, E., Pagé, C., Sauquet, E., Terray, L., Thiéry, D., Oudin, L., Viennot, P., 2013. Impact of climate change on the hydrogeology of two basins in northern France. *Clim. Change* 121, 771–785. <https://doi.org/10.1007/s10584-013-0934-x>.
- Harbaugh, A.W., 2005. MODFLOW 2005, The U. S. geological survey modular groundwater model: the groundwater flow process. *U.S. Geol. Surv. Tech. Methods* 253.
- Hartmann, A., Payeur-Poirier, J.-L., Hopp, L., 2021. Incorporating experimentally derived streamflow contributions into model parameterization to improve discharge prediction. *Hydrol. Earth Syst. Sci. Discuss.* 27, 1325–1341.
- Howard, J., Merrifield, M., 2010. Mapping groundwater dependent ecosystems in California. *PLoS One* 5. <https://doi.org/10.1371/journal.pone.0011249>.
- Huggins, X., Gleeson, T., Serrano, D., Zipper, S., Jehn, F., Rohde, M.M., Abell, R., Vigerstol, K., Hartmann, A., 2023. Overlooked risks and opportunities in groundwater basins of the world's protected areas. *Nat. Sustain.* <https://doi.org/10.1038/s41893-023-01086-9>.
- Institut national de l'information géographique et forestière, 2022. BD TOPO® – La modélisation 2D et 3D du territoire et de ses infrastructures sur l'ensemble du territoire français. [WWW Document]. Géoservices. URL: <https://geoservices.ign.fr/bdtopo> (accessed 1.24.23).
- International convention on Wetlands (Ramsar) [WWW Document], 1971. URL: <http://www.ramsar.org/> (accessed 9.13.23).
- Jasechko, S., Birks, S.J., Gleeson, T., Wada, Y., Fawcett, P.J., Sharp, Z.D., McDonnell, J. J., Welker, J.M., 2014. The pronounced seasonality of global groundwater recharge. *Water Resour. Res.* 50, 8845–8867. <https://doi.org/10.1002/2014WR015809>. Received.
- Jasechko, S., Seybold, H., Perrone, D., Fan, Y., Kirchner, J.W., 2021. Widespread potential loss of streamflow into underlying aquifers across the USA. *Nature* 591, 391–395. <https://doi.org/10.1038/s41586-021-03311-x>.
- Kirchner, J.W., Benettin, P., van Meerveld, I., 2023. Instructive surprises in the hydrological functioning of landscapes. *Annu. Rev. Earth Planet. Sci.* 51. <https://doi.org/10.1146/annurev-earth-071822-100356>.
- Konrad, C.P., 2006. Location and timing of river-aquifer exchanges in six tributaries to the Columbia River in the Pacific Northwest of the United States. *J. Hydrol.* 329, 444–470. <https://doi.org/10.1016/j.jhydrol.2006.02.028>.
- Krakauer, N.Y., Li, H., Fan, Y., 2014. Groundwater flow across spatial scales: Importance for climate modeling. *Environ. Res. Lett.* 9. <https://doi.org/10.1088/1748-9326/9/3/034003>.
- Le Moigne, P., Besson, F., Martin, E., Boé, J., Boone, A., Decharme, B., Etchevers, P., Faroux, S., Habets, F., Lafaysse, M., Leroux, D., Rousset-Regimbeau, F., 2020. The latest improvements with SURFEX v8.0 of the Safran-Isba-Modcou hydrometeorological model for France. *Geosci. Model Dev.* 13, 3925–3946. <https://doi.org/10.5194/gmd-13-3925-2020>.
- Loheide, S.P., Gorelick, S.M., 2007. Riparian hydroecology: a coupled model of the observed interactions between groundwater flow and meadow vegetation patterning. *Water Resour. Res.* 43, 1–16. <https://doi.org/10.1029/2006WR005233>.
- Luo, W., Grudzinski, B.P., Pederson, D., 2010. Estimating hydraulic conductivity from drainage patterns—a case study in the Oregon Cascades. *Geology* 38, 335–338. <https://doi.org/10.1130/G30816.1>.
- Mardhel, V., Pinson, S., Allier, D., 2021. Description of an indirect method (IDPR) to determine spatial distribution of infiltration and runoff and its hydrogeological applications to the French territory. *J. Hydrol.* 592. <https://doi.org/10.1016/j.jhydrol.2020.125609>.
- Martínez-de la Torre, A., Míguez-Macho, G., 2019. Groundwater influence on soil moisture memory and land-atmosphere interactions in the Iberian Peninsula. *Hydrol. Earth Syst. Sci. Discuss.* 1–37. <https://doi.org/10.5194/hess-2018-626>.
- Masson, V., Le Moigne, P., Martin, E., Faroux, S., Alias, A., Alkama, R., Belamari, S., Barbu, A., Boone, A., Bouysse, F., Brousseau, P., Brun, E., Calvet, J.C., Carrer, D., Decharme, B., Delire, C., Donier, S., Essauini, K., Gelbin, A.L., Giordani, H., Habets, F., Jidane, M., Kerdraon, G., Kourzeneva, E., Lafaysse, M., Lafont, S., Lebeaupin Brossier, C., Lemonsu, A., Mahfouf, J.F., Marguinaud, P., Mokhtari, M., Morin, S., Pigeon, G., Salgado, R., Seity, Y., Taillefer, F., Tanguy, G., Tulet, P., Vincendon, B., Vionnet, V., Voldoire, A., 2013. The SURFEXv7.2 land and ocean surface platform for coupled or offline simulation of earth surface variables and fluxes. *Geosci. Model Dev.* 6, 929–960. <https://doi.org/10.5194/gmd-6-929-2013>.
- Maxwell, R.M., Condon, L.E., 2016. Connections between groundwater flow and transpiration partitioning. *Science (80-)* 353, 164–167.
- Maxwell, R.M., Condon, L.E., Kollet, S.J., 2015. A high-resolution simulation of groundwater and surface water over most of the continental US with the integrated hydrologic model ParFlow v3. *Geosci. Model Dev.* 8, 923–937. <https://doi.org/10.5194/gmd-8-923-2015>.
- Messenger, M.L., Lehner, B., Cockburn, C., Lamouroux, N., Pella, H., Snelder, T., Tockner, K., Trautmann, T., Watt, C., Datry, T., 2021. Global prevalence of non-perennial rivers and streams. *Nature* 594, 391–397. <https://doi.org/10.1038/s41586-021-03565-5>.
- Mimeau, L., Künne, A., Branger, F., Kralisch, S., Devers, A., Vidal, J.P., 2024. Flow intermittence prediction using a hybrid hydrological modelling approach: influence of observed intermittence data on the training of a random forest model. *Hydrol. Earth Syst. Sci.* 28, 851–871. <https://doi.org/10.5194/hess-28-851-2024>.
- Muséum national d'Histoire naturelle, 2022. Réseau Natura 2000 – Sites d'importance communautaire désignés par la France [WWW Document]. Inven. Natl. du Patrim. Nat. URL: <https://inpn.mnhn.fr/telechargement/cartes-et-information-geographique/nat/natura> (accessed 9.8.23).
- Muséum national d'Histoire naturelle, 2023a. Zone humide d'importance internationale (convention de Ramsar) [WWW Document]. Inven. Natl. du Patrim. Nat. URL: <https://inpn.mnhn.fr/telechargement/cartes-et-information-geographique/ep/ramsar> (accessed 9.8.23).

- Muséum national d'Histoire naturelle, 2023b. Cartographie nationale milieux humides [WWW Document]. Inven. Natl. du Patrim. Nat. URL <https://inpn.mnhn.fr/telechargement/cartes-et-information-geographique/mh/zh> (accessed 9.5.23).
- National Agency for Biodiversity (OFB), 2023. Indicateurs: Petits cours d'eau asséchés en été [WWW Document]. URL: <https://naturefrance.fr/indicateurs/petits-cours-dea-u-asseches-en-ete>.
- Naz, B.S., Sharples, W., Ma, Y., Goergen, K., Kollet, S., 2023. Continental-scale evaluation of a fully distributed coupled land surface and groundwater model, ParFlow-CLM (v3.6.0), over Europe. *Geosci. Model Dev.* 16, 1617–1639. <https://doi.org/10.5194/gmd-16-1617-2023>.
- Nowak, C., Michon, J., 2017. River flow monitoring in summer. Office Français de la Biodiversité (OFB), 2022. Observatoire national des étiages. [WWW Document]. URL <https://onde.eaufrance.fr/> (accessed 1.23.23).
- Office Français de la Biodiversité (OFB), 2024. French wetland inventory [WWW Document]. URL <https://www.zones-humides.org/actualites/les-nouvelles-donnees-d-inventaires-de-zones-humides-du-rpdzh> (accessed 1.8.24).
- Pasquier, J.-L., 2017. Les prélèvements d'eau douce en France: les grands usages en 2013 et leur évolution depuis 20 ans.
- Quintana-Seguí, P., Le Moigne, P., Durand, Y., Martin, E., Habets, F., Baillon, M., Canellas, C., Franchisteguy, L., Morel, S., 2008. Analysis of near-surface atmospheric variables: validation of the SAFRAN analysis over France. *J. Appl. Meteorol. Climatol.* 47, 92–107. <https://doi.org/10.1175/2007JAMC1636.1>.
- Rapinel, S., Panhelleux, L., Gayet, G., Vanacker, R., Lemercier, B., Laroche, B., Chambaud, F., Guelmami, A., Hubert-Moy, L., 2023. National wetland mapping using remote-sensing-derived environmental variables, archive field data, and artificial intelligence. *Heliyon* 9. <https://doi.org/10.1016/j.heliyon.2023.e13482>.
- Rousset, F., Habets, F., Gomez, E., Le Moigne, P., Morel, S., Noilhan, J., Ledoux, E., 2004. Hydrometeorological modeling of the Seine basin using the SAFRAN-ISBA-MODCCO system. *J. Geophys. Res. D Atmos.* 109, 1–20. <https://doi.org/10.1029/2003JD004403>.
- Saleh, F., Ducharme, A., Flipo, N., Oudin, L., Ledoux, E., 2013. Impact of river bed morphology on discharge and water levels simulated by a 1D Saint-Venant hydraulic model at regional scale. *J. Hydrol.* 476, 169–177. <https://doi.org/10.1016/j.jhydrol.2012.10.027>.
- Sanz, D., Castaño, S., Cassiraga, E., Sahuquillo, A., Gómez-Alday, J.J., Peña, S., Calera, A., 2011. Modeling aquifer-river interactions under the influence of groundwater abstraction in the Mancha Oriental System (SE Spain). *Hydrogeol. J.* 19, 475–487. <https://doi.org/10.1007/s10040-010-0694-x>.
- Sauquet, E., Beaufort, A., Sarremejane, R., Thirel, G., 2021. Predicting flow intermittence in France under climate change. *Hydrol. Sci. J.* 66, 2046–2059. <https://doi.org/10.1080/02626667.2021.1963444>.
- Scanlon, B.R., Fakhreddine, S., Rateb, A., de Graaf, I., Famiglietti, J., Gleeson, T., Grafton, R.Q., Jobbagy, E., Kebede, S., Kolusu, S.R., Konikow, L.F., Long, D., Mekonnen, M., Schmied, H.M., Mukherjee, A., MacDonald, A., Reedy, R.C., Shamsudduha, M., Simmons, C.T., Sun, A., Taylor, R.G., Villholth, K.G., Vörösmarty, C.J., Zheng, C., 2023. Global water resources and the role of groundwater in a resilient water future. *Nat. Rev. Earth Environ.* 2023 (4), 1–15. <https://doi.org/10.1038/s43017-022-00378-6>.
- Schaller, M.F., Fan, Y., 2009. River basins as groundwater exporters and importers: implications for water cycle and climate modeling. *J. Geophys. Res. Atmos.* 114. <https://doi.org/10.1029/2008JD010636>.
- Schuite, J., Flipo, N., Massei, N., Rivière, A., Baratelli, F., 2019. Improving the spectral analysis of hydrological signals to efficiently constrain watershed properties. *Water Resour. Res.* 55, 4043–4065. <https://doi.org/10.1029/2018WR024579>.
- Shanfield, M., Bourke, S.A., Zimmer, M.A., Costigan, K.H., 2021. An overview of the hydrology of non-perennial rivers and streams. *Wiley Interdiscip. Rev. Water* 8, 1–25. <https://doi.org/10.1002/wat2.1504>.
- Simon, N., Bour, O., Fauchoux, M., Lavenant, N., Lay, H. Le, Fovet, O., Thomas, Z., Longuevergne, L., 2022. Combining passive and active distributed temperature sensing measurements to locate and quantify groundwater discharge variability into a headwater stream 1459–1479.
- Sobaga, A., Decharme, B., Habets, F., Delire, C., Enjelvin, N., Redon, P., Faure-cattelain, P., Moigne, P.L., 2023a. Assessment of the ISBA Land Surface Model soil hydrology using four closed-form soilwater relationships and several lysimeters. *Hydrol. Earth Syst. Sci. Process.* 27, 2437–2461.
- Sobaga, A., Habets, F., Beaudoin, N., Léonard, J., Decharme, B., 2023b. Decreasing trend of groundwater recharge with limited impact of intense precipitation: evidence from long-term lysimeter data. <https://doi.org/10.2139/ssrn.4613998>.
- Sophocleous, M., 2000. From safe yield to sustainable development of water resources – the Kansas experience. *J. Hydrol.* 235, 27–43. [https://doi.org/10.1016/S0022-1694\(00\)00263-8](https://doi.org/10.1016/S0022-1694(00)00263-8).
- Stoll, S., Weiler, M., 2010. Explicit simulations of stream networks to guide hydrological modelling in ungauged basins. *Hydrol. Earth Syst. Sci.* 14, 1435–1448. <https://doi.org/10.5194/hess-14-1435-2010>.
- Taniguchi, M., Burnett, W.C., Cable, J.E., Turner, J.V., 2002. Investigation of submarine groundwater discharge. *Hydrol. Process.* 16, 2115–2129. <https://doi.org/10.1002/hyp.1145>.
- Therrien, R., McLaren, R.G., Sudicky, E.A., Panday, S.M., 2010. HydroGeoSphere: a three-dimensional numerical model describing fully-integrated subsurface and surface flow and solute transport. Groundwater Simulations Group, Waterloo, Ont., Canada. <https://doi.org/10.1111/j.1745-6584.2011.00882.x>.
- Thierion, C., Longuevergne, L., Habets, F., Ledoux, E., Ackerer, P., Majdalani, S., Leblais, E., Lecluse, S., Martin, E., Queguiner, S., Viennot, P., 2012. Assessing the water balance of the Upper Rhine Graben hydrosystem. *J. Hydrol.* 424–425, 68–83. <https://doi.org/10.1016/j.jhydrol.2011.12.028>.
- Thiéry, D., 2015. Code de calcul MARTHE – Modélisation 3D des écoulements et des transferts dans les hydrosystèmes – Notice d'utilisation de la version 7.5. (MARTHE: Modeling software for groundwater flows), BRGM/RP-64554-FR. Orléans.
- Tramblay, Y., Rutkowska, A., Sauquet, E., Sefton, C., Laaha, G., Osuch, M., Albuquerque, T., Alves, M.H., Banasik, K., Beaufort, A., Brocca, L., Camici, S., Csabai, Z., Dakhlaoui, H., DeGirolo, A.M., Dörfinger, G., Gallart, F., Gauster, T., Hanich, L., Kohnová, S., Mediero, L., Plamen, N., Parry, S., Quintana-Seguí, P., Tzoraki, O., Detry, T., 2021. Trends in flow intermittence for European rivers. *Hydrol. Sci. J.* 66, 37–49. <https://doi.org/10.1080/02626667.2020.1849708>.
- Vergnes, J.P., Decharme, B., Habets, F., 2014. Introduction of groundwater capillary rises using subgrid spatial variability of topography into the ISBA land surface model. *J. Geophys. Res.* 119, 11065–11086. <https://doi.org/10.1002/2014JD021573>.
- Vergnes, J.P., Habets, F., 2018. Impact of river water levels on the simulation of stream-aquifer exchanges over the Upper Rhine alluvial aquifer (France/Germany). *Hydrogeol. J.* 26, 2443–2457. <https://doi.org/10.1007/s10040-018-1788-0>.
- Vergnes, J.P., Roux, N., Habets, F., Ackerer, P., Amraoui, N., Besson, F., Caballero, Y., Courtois, Q., De Dreuzy, J.R., Etchevers, P., Gallois, N., Leroux, D.J., Longuevergne, L., Le Moigne, P., Morel, T., Munier, S., Regimbeau, F., Thiéry, D., Viennot, P., 2020. The AquifR hydrometeorological modelling platform as a tool for improving groundwater resource monitoring over France: evaluation over a 60-year period. *Hydrol. Earth Syst. Sci.* 24, 633–654. <https://doi.org/10.5194/hess-24-633-2020>.
- Winter, T.C., 1999. Relation of streams, lakes, and wetlands to groundwater flow systems. *Hydrogeol. J.* 7, 28–45. <https://doi.org/10.1007/s100400050178>.
- Xanke, J., Liesch, T., 2022. Quantification and possible causes of declining groundwater resources in the Euro-Mediterranean region from 2003 to 2020. *Hydrogeol. J.* 30, 379–400. <https://doi.org/10.1007/s10040-021-02448-3>.
- Zedler, J.B., Kercher, S., 2005. WETLAND RESOURCES: status, trends, ecosystem services, and restorability. *Annu. Rev. Environ. Resour.* 30, 39–74. <https://doi.org/10.1146/annurev.energy.30.050504.144248>.
- Zimmer, M.A., McGlynn, B.L., 2017. Ephemeral and intermittent runoff generation processes in a low relief, highly weathered catchment. *Water Resour. Res.* 53, 7055–7077. <https://doi.org/10.1002/2016WR019742>.
- Zipper, S., Brookfield, A., Ajami, H., Ayers, J.R., Beightel, C., Fienen, M.N., Gleeson, T., Hammond, J., Hill, M., Kendall, A.D., Kerr, B., Lapidés, D., Porter, M., Parimalarenganayaki, S., Rohde, M.M., Wardropper, C., 2024. Streamflow depletion caused by groundwater pumping: fundamental research priorities for management-relevant science. *Water Resour. Res.* 60, 1–7. <https://doi.org/10.1029/2023WR035727>.